



Year: 2011

Mammalian soluble epoxide hydrolase is identical to liver hepoxilin hydrolase

Cronin, A; Decker, M; Arand, M

Abstract: Hepoxilins are lipid signaling molecules derived from arachidonic acid through the 12-lipoxygenase pathway. These trans-epoxy hydroxy eicosanoids play a role in a variety of physiological processes, including inflammation, neurotransmission, and formation of skin barrier function. Mammalian hepoxilin hydrolase, partly purified from rat liver, has earlier been reported to degrade hepoxilins to trioxilins. Here, we report that hepoxilin hydrolysis in liver is mainly catalyzed by soluble epoxide hydrolase (sEH): i) purified mammalian sEH hydrolyses hepoxilin A and B with a V(max) of 0.4-2.5 mol/mg/min; ii) the highly selective sEH inhibitors N-adamantyl-N'-cyclohexyl urea and 12-(3-adamantan-1-yl-ureido) dodecanoic acid greatly reduced hepoxilin hydrolysis in mouse liver preparations; iii) hepoxilin hydrolase activity was abolished in liver preparations from sEH(-/-) mice; and iv) liver homogenates of sEH(-/-) mice show elevated basal levels of hepoxilins but lowered levels of trioxilins compared with wild-type animals. We conclude that sEH is identical to previously reported hepoxilin hydrolase. This is of particular physiological relevance because sEH is emerging as a novel drug target due to its major role in the hydrolysis of important lipid signaling molecules such as epoxyeicosatrienoic acids. sEH inhibitors might have undesired side effects on hepoxilin signaling.

DOI: <https://doi.org/10.1194/jlr.M009639>

Posted at the Zurich Open Repository and Archive, University of Zurich

ZORA URL: <https://doi.org/10.5167/uzh-54382>

Journal Article

Accepted Version

Originally published at:

Cronin, A; Decker, M; Arand, M (2011). Mammalian soluble epoxide hydrolase is identical to liver hepoxilin hydrolase. *Journal of Lipid Research*, 52(4):712-719.

DOI: <https://doi.org/10.1194/jlr.M009639>

Mammalian soluble epoxide hydrolase is identical to liver hepoxilin hydrolase

Annette Cronin*, Martina Decker and Michael Arand

Institute of Pharmacology and Toxicology, University of Zurich, Winterthurer Str 190, 8057 Zurich, Switzerland,

Running title: Role of soluble epoxide hydrolase in hepoxilin metabolism.

Correspondence to: Dr. Annette Cronin, Institute of Pharmacology and Toxicology, University of Zurich, Winterthurer Str 190, CH-8057 Zurich, Switzerland. Tel: +41 44 63 55979; Fax: +41 44 63 55979; E-mail: cronin@pharma.uzh.ch

Abbreviations: ACU, N-adamantyl-N'-cyclohexyl urea; AUDA, 12-(3-adamantan-1-yl-ureido) dodecanoic acid; EETs, epoxyeicosatrienoic acids; Hx, hepoxilin; sEH, epoxide hydrolase; Hepoxilin Hydrolase, Hepoxilin A₃ epoxide hydrolase; EDHF, endothelium derived hyperpolarising factor; 12-LOX, 12-lipoxygenase; eLOX-3, epidermis-type lipoxygenase 3.

Abstract

Hepoxilins are lipid signalling molecules derived from arachidonic acid through the 12-lipoxygenase pathway. These *trans*-epoxy hydroxy eicosanoids play a role in a variety of physiological processes, including inflammation, neurotransmission and formation of skin barrier function. Mammalian hepoxilin hydrolase - partly purified from rat liver - has earlier been reported to degrade hepoxilins to trioxilins. Here, we report that hepoxilin hydrolysis in liver is mainly catalysed by soluble epoxide hydrolase (sEH). (i) Purified mammalian sEH hydrolyses hepoxilin A₃ and B₃ with a V_{max} of 0.4 – 2.5 μmol/mg/min, (ii) the highly selective sEH inhibitors N-adamantyl-N'-cyclohexyl urea (ACU) and 12-(3-adamantan-1-yl-ureido) dodecanoic acid (AUDA) greatly reduced hepoxilin hydrolysis in mouse liver preparations; (iii) hepoxilin hydrolase activity was abolished in liver preparations from sEH^{-/-} mice and (iv) liver homogenates of sEH^{-/-} mice show elevated basal level of hepoxilins but lowered levels of trioxilins compared to WT animals. We conclude that sEH is identical to previously reported hepoxilin hydrolase. This is of particular physiological relevance because sEH is emerging as a novel drug target, due to its major role in the hydrolysis of important lipid signalling molecules such as epoxyeicosatrienoic acids (EETs). sEH inhibitors might have undesired side effects on hepoxilin signalling.

Supplementary key words: soluble epoxide hydrolase, hepoxilin hydrolase, lipid metabolism, hepoxilin, 12-LOX.

Introduction

Epoxide hydrolases (EC 3.3.2.7-11) catalyse the hydrolysis of oxiranes to the corresponding vicinal diols. To date a number of mammalian epoxide hydrolases are characterized that play diverse roles in the organism (1).

The soluble epoxide hydrolase (sEH, EC 3.1.3.76; EC 3.3.2.10) is a bifunctional, homodimeric enzyme composed of an epoxide hydrolase (EH) and a lipid phosphatase in each of its subunits (2-4). The sEH is abundantly expressed throughout the organism (5, 6) and accepts a broad range of substrates (7, 8), in particular endogenous epoxides derived from unsaturated fatty acids such as epoxyeicosatrienoic acids (EETs) (9). The organism utilises these lipid epoxides as important signalling molecules which regulate a variety of physiological functions. EETs were identified as endothelium derived hyperpolarizing factors (EDHF) (10) acting on vascular smooth muscle cells leading to hyperpolarization and vasodilation (11, 12). Since then several experimental hypertensive models confirmed a role for EETs in blood pressure regulation and end organ protection (13, 14). EETs further have antiinflammatory and antinociceptive properties (15-17) and finally seem to promote cell proliferation, migration and angiogenesis (18-20).

The metabolism of these lipid epoxides by sEH to the corresponding diols is generally considered a deactivation process. For this reason the sEH is a promising target for the treatment of hypertension, inflammatory diseases, pain, diabetes and stroke (16, 21-25). A number of sEH inhibitors (sEHI) have been developed (26, 27) for therapeutic applications. Yet, the sEH also serves some function in xenobiotic metabolism by accepting certain *trans*-substituted epoxides, which are very poor substrates for microsomal epoxide hydrolase (mEH) (28, 29).

Other epoxide hydrolases with rather narrow substrate selectivity have been identified in mammals. Of those, Hepoxilin A₃ epoxide hydrolase (Hepoxilin hydrolase, EC 3.3.2.7) was

partly purified from rat liver cytosol and identified as the main hydrolase of the endogenous lipid hepoxilin A₃. The authors further discriminated hepoxilin hydrolase from other EHs due to its size (53 kDa) and substrates preference for hepoxilin A₃, compared to leukotriene or styrene oxide (30). To date, the enzyme is only incompletely characterized and no structural or sequence information is available.

Most enzymatic derived endogenous lipid epoxides are of *cis*-configuration, but also some *trans*-substituted lipid epoxides are formed within the organism, such as the inflammatory mediator leukotriene A₄. The *trans*-epoxy hydroxy eicosanoids hepoxilin A₃ and B₃ (HxA₃ and HxB₃) are formed from arachidonic acid through the 12-lipoxygenase pathway (figure 1) in various organs like liver, brain, lung, pancreas and skin (9, 31). They can be transformed to the corresponding trihydroxy metabolites (trioxilins, Trx) or glutathione conjugates (32).

Early studies showed an hepoxilin mediated increased insulin release from pancreatic islets (33). In the brain hepoxilins modulate synaptic neurotransmission and neuronal excitability - mostly through stimulation of intracellular calcium release or increased calcium influx into the cell (34-37). Hepoxilin are considered pro-inflammatory because increased hepoxilins and trioxilin levels have been found in psoriatic lesions (38) and hepoxilin A₃ was shown to regulate neutrophil migration in response to inflammation (39, 40). Several reports suggest an involvement of these lipid mediators in epidermal differentiation and skin barrier function (41). Interestingly, mutations in the hepoxilin generating 12R-LOX pathway in the skin are associated with a congenital form of ichthyosis (42-46). A hepoxilin receptor has not been identified, but several reports (34, 47-49) support its existence.

Here, we report that 12S-LOX derived hepoxilin A₃ and B₃ (HxA₃ and HxB₃), are efficiently converted to the corresponding trihydroxy metabolites (trioxilins) by soluble epoxide hydrolases (sEH). Our results suggest a biological relevance of sEH - rather than hepoxilin hydrolase - in hepoxilin metabolism, which opens a new branch in the numerous physiological functions of sEH.

Methods

Enzyme Assays. Human full length sEH containing an N-terminal Strep-Tag and rat sEH containing an N-terminal His-Tag were cloned, recombinantly expressed in *E.coli* and purified as described previously (3). Epoxide hydrolase activity was measured using 8(R,S)-Hydroxy-11S,12S-epoxyeicosa-5Z,9E,14Z-trienoic acid (HxA₃) and 10(R,S)-Hydroxy-11S,12S-epoxyeicosa-5Z,8Z,14Z-trienoic acid (HxB₃) as substrates by determining the formation of the corresponding diols 8(R,S)-Hydroxy-11,12-dihydroxyeicosa-5Z,9E,14Z-trienoic acid (TxA₃) and 10(R,S)-Hydroxy-11,12-dihydroxyeicosa-5Z,8Z,14Z-trienoic acid (TxB₃). Typically, 5-50 ng purified sEH or 10 - 100 µg organ extracts were incubated with various concentrations HxA₃ and HxB₃ ranging from 0.1-30 µM with or without inhibitors in 50 mM Tris HCl, 50 mM NaCl, 2 % glycerol, pH 7.4 in a final volume of 50 µl for 10 min at 37°C. The reaction was stopped by addition of 2 volumes of methanol and samples were pelleted for 5 min at 13.000 rpm prior to LC-MS/MS analysis. Substrate turnover was determined using internal HxA₃ and HxB₃ standards. EH activity against epoxyeicosatrienoic acids (EETs) was performed as described previously (50). Kinetic constants were calculated by kinetic modelling based on the equation $V = E \times CS / (CS + K_m)$ (with $V = \% \text{ turnover of } V_{\max}$, $E = \text{total amount of enzyme}$, $CS = \text{substrate concentration}$, and $K_m = \text{Michaelis Menten constant}$). Variations were calculated from 4-5 independent experiments using freshly prepared enzyme preparations.

Lipid substrates were purchased from Biomol except for TxA₃ and TxB₃, which were synthesized biochemically using purified soluble epoxide hydrolase. One µg HxA₃ or HxB₃ were turned over to the corresponding diol using 200 ng soluble epoxide hydrolase in 50 mM Tris HCl, 50 mM NaCl, 2 % glycerol, pH 7.4 in a final volume of 500 µl for 30 min at 37°C. The reaction products were extracted trice with 2 volumes of ethyl acetate, dried under a stream of nitrogen and reconstituted in methanol.

LC-MS/MS analysis. Separation of analytes was performed on an Agilent eclipse XDB-C18 reverse phase column (4.6 x 150 mm, 5 μ m pore size) with a corresponding opti-gard pre-column using an Agilent 1100 liquid chromatography system. The mobile phase consisted of (A) 0.1% formic acid and (B) acetonitrile containing 0.1% formic acid at a flow rate of 400 μ l/min using an injection volume of 20 μ l. Starting conditions of 70% buffer B were maintained for 2 min, followed by a linear gradient from 70 to 100% B within 7 min. An isocratic flow of 100% B was held for 1.5 min and finally the column was re-equilibrated for 2 min with 70% B. The HPLC system was coupled to a 4000 QTRAP hybrid quadrupole linear ion trap mass spectrometer (Applied Biosystems) equipped with a TurboV source and electrospray (ESI) interface. Analytes were recorded using multiple reaction monitoring in negative mode (-MRM) using the following source specific parameters: IS -4500V, TEM 450°C, curtain gas (CUR = 30), nebulizer gas (GS1 = 50), heater gas (GS2 = 70) and collision gas (CAD = 10). The compound specific parameters for the different substrates (as specified in supplemental material) were determined by direct infusion of standard solutions (100-300 ng/ml) in methanol at a flow rate of 10 μ l/min using the quantitative optimization function of the Analyst software 1.4.2. Samples were quantified by determining the peak AUC with the quantification function of the Analyst software 1.4.2 using the transitions as specified in supplemental material. The background noise was assessed by analysing blank samples and standard curves were generated using blank samples spiked with a series of control lipids ranging from 1-1000 ng/ml. For HxA₃, HxB₃, TxA₃ and TxB₃ the limit of detection (LOD) ranged from 4 to 20 pg and the limit of quantification (LOQ) from 15-65 pg, corresponding to a signal-to-noise ratio of 3 and 10, respectively.

Organ extracts. C57BL/6 mice were obtained from the Institute of Laboratory Animal Sciences University of Zurich and C57BL/6 sEH^{-/-} mice (51) were kindly provided by Dr. F.J. Gonzales (NIH, Bethesda, MD, USA). 6-10 week old male mice were sacrificed by cervical

dislocation, and livers were excised and homogenized in ice-cold phosphate buffered saline, pH 7.4. All subsequent steps were performed at 4°C. Cytosolic and microsomal fractions were prepared by ultracentrifugation of the 9000 x g supernatant of the liver homogenates at 100.000 x g for 45 min.

Lipid extracts. Lipids were extracted from liver homogenates by addition of ethanol to a final concentration of 25%, followed by solid phase extraction on C18 Bond Elut SPE columns (Varian, Palo Alto, CA, USA). Extracts were applied to the SPE columns preconditioned with 2 ml acetonitrile and 2 ml ddH₂O. Columns were washed with 1 ml ddH₂O and evaporated to dryness. Lipids were eluted with 3 x 600 µl ethylacetate, dried under a stream of nitrogen, dissolved in acetonitrile, and pelleted for 2 min at 13.000 rpm prior to LC-MS/MS analysis as described above. In some cases liver homogenates were treated with 30 µM arachidonic acid at 37 °C for 30 min and lipids were isolated by solid phase extraction as described above.

Western Blot. Protein samples in Laemmli buffer were subjected to SDS-polyacrylamide gel electrophoresis and semi-dry blotting following standard procedures. Blots were incubated with polyclonal sEH rabbit antiserum for 2 hours (dilution of 1:1000) in Tris-buffered saline containing 0.5% Tween-20. An alkaline phosphatase conjugated anti-rabbit antibody (Sigma Aldrich) was applied at a dilution of 1:30000 followed by colorimetric detection using BCIP and NBT.

Results

Soluble epoxide hydrolase efficiently turns over hepoxilin A₃ and B₃. Human and rat sEH were cloned, recombinantly expressed in *E.coli* and purified to homogeneity using affinity chromatography as described previously (3). To determine the effect of purified recombinant rat or human sEH on hepoxilin metabolism we used LC-MS/MS analysis followed by kinetic evaluation. Human or rat sEH was incubated with various concentrations of HxA₃ and HxB₃ with or without inhibitors and samples were analysed by LC-MS/MS. HxA₃ is efficiently hydrolysed by purified rat soluble epoxide hydrolase with a V_{max} of 1.7 μmol/mg/min, a K_m of 5 μM and a catalytic efficiency of 4.5 x 10⁵ as shown in figure 2. Both HxA₃ and HxB₃ are substrates for purified rat sEH and also human sEH (figure 2) and a summary of the kinetic parameters is presented in table 1.

Hepoxilin hydrolase activity is linked to sEH presence. To evaluate the physiological contribution of sEH to hepoxilin metabolism, we separated mouse liver cytosolic fractions using gel permeation chromatography and tested each elution fraction for the metabolism of HxA₃, 14,15-EET and 5,6-EET. Each fraction was further assayed for the presence of sEH by western blot analysis (figure 3). The hepoxilin hydrolase and sEH activities show 100% co-elution from the column. Moreover, the fraction with the highest hepoxilin hydrolase activity also contains the highest amount of sEH (figure 3, lower panel).

Hepoxilin turnover is inhibited by sEH but not mEH inhibitors. To characterise the physiological contribution of sEH to hepoxilin metabolism, we used a selection of epoxide hydrolase inhibitors. The hepoxilin turnover by purified sEH was effectively inhibited by sEHIs as shown in figure 4. Hepoxilin metabolism in liver protein extracts from WT animals was inhibited by ACU and AUDA but not the mEH inhibitor valpromide, as shown in figure

5. In addition, ACU inhibited hepoxilin metabolism by purified rat sEH and liver cytosolic preparations with an IC_{50} value of approximately 1 nM (data not shown), which is in line with previously reported data (52). In microsomal preparations of sEH WT mice hepoxilin turnover amounted to 30% compared to the cytosolic fraction. Western blot analysis of microsomal and cytosolic liver preparations confirmed the presence of sEH protein in both liver fractions, although to significantly lower amount in microsomes (data not shown). Furthermore, purified microsomal epoxide hydrolase which is highly abundant in the liver does not show any activity against hepoxilins (data not shown).

sEH is responsible for hepoxilin metabolism. To investigate the quantitative contribution of sEH to hepoxilin turnover we incubated protein extracts isolated from livers of sEH WT and sEH^{-/-} mice with HxA₃ and HxB₃. Hepoxilin turnover to trioxilins was greatly abolished in sEH^{-/-} mice compared to the WT mice (figure 6). Specifically, in both cytosolic and microsomal liver preparations of sEH^{-/-} mice, the activity towards HxA₃ and HxB₃ was greatly reduced compared to the WT mice. Again, the activity towards hepoxilins in liver microsomal preparations of WT animals is explained by the presence of some sEH, while no sEH protein was detectable in the sEH^{-/-} mice by immunoblotting (data not shown).

Hepoxilin/trioxilin contents of livers of WT and sEH^{-/-} mice *in vivo*. Lipids were extracted from liver organ preparations of sEH WT and sEH^{-/-} mice with or without pre-treatment with arachidonic acid followed by LC-MS/MS analysis of the lipids. Liver homogenates of sEH^{-/-} mice show a significantly elevated basal level of hepoxilin B₃ but lowered levels of trioxilins compared to the WT animals (figure 7a), where trioxilins are readily formed. After arachidonic acid treatment of organ extract the synthesis of hepoxilin precursors is greatly induced (40fold) and the accumulation of hepoxilins in liver homogenates from sEH^{-/-} mice is even more pronounced (figure 7b).

Discussion

Here we report for the first time that *trans*-hydroxy-epoxy lipids, in particular the endogenous 12S-LOX derived lipid mediators HxA₃ and HxB₃ are excellent substrates for mammalian sEH and converted to the corresponding trioxilins. 12R-LOX derived hepoxilins which are specifically generated in skin are most likely preferred sEH substrates, although they have not been tested to date. sEH metabolises hepoxilins with a catalytic efficiency which is within the range of turnover of its previously identified physiological substrates epoxyeicosatrienoic acids (EETs) which are among the best endogenous substrates for sEH. The activity of mammalian sEH against EETs lies in the range of 1-20 μmol/mg/min. We do not see a negative cooperativity with both hepoxilins, like it has been suggested for the EET turnover by sEH (50). Human sEH turns over hepoxilins less efficiently (by a factor of three) than rat sEH. This has been seen for other substrates and might be explained by a compensatory effect due to the lower expression level of sEH in rat liver compared to human liver. HxA₃ is a better substrate for mammalian sEH than HxB₃. The hydroxy group positioned directly next to the epoxide might pose a sterical hindrance leading to less efficient turnover by sEH.

The sEH turns over hepoxilins orders of magnitudes more efficiently than the previously reported hepoxilin hydrolase that displayed a specific activity of 0.2 nmol/mg/min. Hepoxilin hydrolase was partly purified from rat liver and suggested to be distinct from other mammalian EHs (mEH, sEH, Leukotriene A₄ Hydrolase) by its molecular weight as well as substrate and inhibitor spectrum. However, hepoxilin hydrolase is still only incompletely characterized and the amino acid sequence is not reported to date. The purification scheme used for the isolation of hepoxilin hydrolase (30) is quiet similar to the procedure used for the isolation of rat liver sEH (53). We assume that the hepoxilin hydrolase activity in the enzyme preparation published previously is due to an invisible contamination by sEH. The assignment

of the enzymatic activity to an incorrect polypeptide might be due to the obviously low abundance of sEH in livers of untreated rats, which would also explain the striking activity difference between the two enzymes.

These results suggested a physiological role of sEH in hepoxilin metabolism. Analysis of mouse liver cytosol by gel permeation chromatography followed by activity measurements against HxA3, 14,15-EET (an excellent sEH substrate) and 5,6-EET (a rather poor sEH substrate) and western blot revealed that the hepoxilin hydrolase activity is linked to sEH presence, showing a perfect match. The double peak in the activity profile can be explained by the presence of monomeric and dimeric sEH in liver cytosol. These results suggested that mammalian sEH – rather than hepoxilin hydrolase - is the key enzyme responsible for hepoxilin metabolism in mouse liver.

To strengthen our hypothesis we analysed liver extracts from sEH WT and sEH^{-/-} mice. Hepoxilin turnover was greatly abolished compared to the WT animals. The activity against hepoxilins found in the liver microsomal preparation of WT animals can be explained by the presence of sEH due to its partial peroxisomal localisation in liver (54, 55), which we confirmed by western blot analysis.

Only sEHs but not mEHs quantitatively inhibited hepoxilin turnover in cytosolic as well as microsomal liver preparations of WT animals. mEH shows a substrate preference for bulky, *cis*-substituted epoxides compared to the sEH, which accepts both *cis*- and *trans*-substituted epoxides. Indeed, we have shown that purified microsomal epoxide hydrolase does not turnover hepoxilins. In addition, ACU inhibited hepoxilin metabolism by purified rat sEH as well as liver cytosolic preparations with an IC₅₀ value of approximately 1 nM. These results are further supported by the LC-MS/MS analysis of lipid fractions prepared from organs of sEH WT and sEH^{-/-} animals. The liver homogenates of sEH^{-/-} mice show elevated basal levels of hepoxilins, particularly HxB₃, while trioxilins levels are significantly decreased compared to the WT animals (figure 7a). The pre-treatment of organ extracts with arachidonic

acid (AA) presumably leads to a strong production of hepoxilin precursors such as 12HPETE. In this case, both HxA₃ and HxB₃ significantly accumulate in the livers of sEH^{-/-} animals and only a slow turnover to trioxilins is detected (figure 7b). An AA pre-treatment better reflects the actual enzyme capacity of the organ analysed, while in the basal state compensatory mechanisms of lipid metabolism might be of importance.

Quite unexpected were the large amounts of particularly HxB₃ in the livers of sEH^{-/-} mice while HxA₃ did not accumulate to that extent. HxA₃ has been shown to be a substrate for glutathione-S-transferases, and the glutathione conjugated metabolite maintains biologic activity (32, 37). Due to the high expression level of GSTs in the liver, one would expect a lack of hepoxilin accumulation, which is only seen for the HxA₃ regioisomer (figure 7). Therefore glutathione conjugation of HxB₃ does not seem to be an important pathway in the liver. Note that the glutathione derivative of HxB₃ has not been detected *in vivo* to date. In contrast, HxA₃ seem to be preferentially glutathionylated in livers of sEH^{-/-} animals, which might also be the case in other organs, when the epoxide hydrolysis pathway is blocked.

Taken together our results strongly suggest that mammalian sEH is the key enzyme responsible for hepoxilin metabolism and indeed identical to previously reported hepoxilin hydrolase. Other mammalian epoxide hydrolase contribute – if at all – only partly to this metabolic pathway, depending on the tissue analysed.

Our inhibitory analyses using sEHI clearly show a complete block of hepoxilin hydrolysis in the liver. Therefore possible undesirable effects of sEH inhibitors, which are in development for a number of applications, should be considered. Lipid signalling pathways other than the mostly targeted EET pathways might be affected, with – to our knowledge – unknown consequences. This is even more important as EETs and hepoxilins seem to have somewhat opposing effects. While the action of EETs are generally considered anti-inflammatory (15-17), hepoxilins instead are suspected to have pro-inflammatory effects. In psoriatic lesions elevated levels of hepoxilins and trioxilins have been detected (38).

Furthermore, hepoxilin A₃ has recently been identified as pathogen elicited epithelial chemoattractant (PEEC). HxA₃ leads to neutrophil migration across epithelial barriers in response to mucosal inflammation in the intestine or lung (39, 40). An inhibition of sEH might therefore cause enhanced release of hepoxilins at inflammatory sites. Such a deregulation might trigger pathophysiological effect of inflammation seen for example in inflammatory bowel disease, cystic fibrosis or chronic obstructive pulmonary disease of the lung.

In conclusion, hepoxilins are excellent substrates for mammalian sEH *in vitro* and *in vivo*. Our findings suggest that sEH is identical to liver hepoxilin hydrolase and plays an important role in the physiological regulation of hepoxilins, with important implications in particular for inflammatory diseases.

Acknowledgements

The financial support by the Swiss National Science Foundation (MA, No. 3100A0-108326) is greatly acknowledged. Some of the work described herein is part of the PhD thesis of Martina Decker. We cordially thank Julia Burgener for providing purified microsomal epoxide hydrolase.

References

- (1) Decker, M., Arand, M., and Cronin, A. (2009) Mammalian epoxide hydrolases in xenobiotic metabolism and signalling. *Arch Toxicol* 83, 297-318.
- (2) Cronin, A., Homburg, S., Durk, H., Richter, I., Adamska, M., Frere, F., and Arand, M. (2008) Insights into the catalytic mechanism of human sEH phosphatase by site-directed mutagenesis and LC-MS/MS analysis. *J Mol Biol* 383, 627-40.
- (3) Cronin, A., Mowbray, S., Durk, H., Homburg, S., Fleming, I., Fisslthaler, B., Oesch, F., and Arand, M. (2003) The N-terminal domain of mammalian soluble epoxide hydrolase is a phosphatase. *Proc Natl Acad Sci U S A* 100, 1552-7.
- (4) Newman, J. W., Morisseau, C., Harris, T. R., and Hammock, B. D. (2003) The soluble epoxide hydrolase encoded by EPXH2 is a bifunctional enzyme with novel lipid phosphate phosphatase activity. *Proc Natl Acad Sci U S A* 100, 1558-63.
- (5) Enayetallah, A. E., French, R. A., Thibodeau, M. S., and Grant, D. F. (2004) Distribution of soluble epoxide hydrolase and of cytochrome P450 2C8, 2C9, and 2J2 in human tissues. *J Histochem Cytochem* 52, 447-54.
- (6) Sura, P., Sura, R., Enayetallah, A. E., and Grant, D. F. (2008) Distribution and expression of soluble epoxide hydrolase in human brain. *J Histochem Cytochem* 56, 551-9.
- (7) Summerer, S., Hanano, A., Utsumi, S., Arand, M., Schuber, F., and Blee, E. (2002) Stereochemical features of the hydrolysis of 9,10-epoxystearic acid catalysed by plant and mammalian epoxide hydrolases. *Biochem J* 366, 471-80.
- (8) Zeldin, D. C., Kobayashi, J., Falck, J. R., Winder, B. S., Hammock, B. D., Snapper, J. R., and Capdevila, J. H. (1993) Regio- and enantiofacial selectivity of epoxyeicosatrienoic acid hydration by cytosolic epoxide hydrolase. *J Biol Chem* 268, 6402-7.

- (9) Newman, J. W., Morisseau, C., and Hammock, B. D. (2005) Epoxide hydrolases: their roles and interactions with lipid metabolism. *Prog Lipid Res* 44, 1-51.
- (10) Fisslthaler, B., Popp, R., Kiss, L., Potente, M., Harder, D. R., Fleming, I., and Busse, R. (1999) Cytochrome P450 2C is an EDHF synthase in coronary arteries. *Nature* 401, 493-7.
- (11) Hu, S., and Kim, H. S. (1993) Activation of K⁺ channel in vascular smooth muscles by cytochrome P450 metabolites of arachidonic acid. *Eur J Pharmacol* 230, 215-21.
- (12) Li, P. L., and Campbell, W. B. (1997) Epoxyeicosatrienoic acids activate K⁺ channels in coronary smooth muscle through a guanine nucleotide binding protein. *Circ Res* 80, 877-84.
- (13) Imig, J. D., Zhao, X., Capdevila, J. H., Morisseau, C., and Hammock, B. D. (2002) Soluble epoxide hydrolase inhibition lowers arterial blood pressure in angiotensin II hypertension. *Hypertension* 39, 690-4.
- (14) Zhao, X., Yamamoto, T., Newman, J. W., Kim, I. H., Watanabe, T., Hammock, B. D., Stewart, J., Pollock, J. S., Pollock, D. M., and Imig, J. D. (2004) Soluble epoxide hydrolase inhibition protects the kidney from hypertension-induced damage. *J Am Soc Nephrol* 15, 1244-53.
- (15) Inceoglu, B., Jinks, S. L., Schmelzer, K. R., Waite, T., Kim, I. H., and Hammock, B. D. (2006) Inhibition of soluble epoxide hydrolase reduces LPS-induced thermal hyperalgesia and mechanical allodynia in a rat model of inflammatory pain. *Life Sci*.
- (16) Schmelzer, K. R., Inceoglu, B., Kubala, L., Kim, I. H., Jinks, S. L., Eiserich, J. P., and Hammock, B. D. (2006) Enhancement of antinociception by coadministration of nonsteroidal anti-inflammatory drugs and soluble epoxide hydrolase inhibitors. *Proc Natl Acad Sci U S A* 103, 13646-51.
- (17) Smith, K. R., Pinkerton, K. E., Watanabe, T., Pedersen, T. L., Ma, S. J., and Hammock, B. D. (2005) Attenuation of tobacco smoke-induced lung inflammation by

- treatment with a soluble epoxide hydrolase inhibitor. *Proc Natl Acad Sci U S A* 102, 2186-91.
- (18) Michaelis, U. R., Fisslthaler, B., Barbosa-Sicard, E., Falck, J. R., Fleming, I., and Busse, R. (2005) Cytochrome P450 epoxygenases 2C8 and 2C9 are implicated in hypoxia-induced endothelial cell migration and angiogenesis. *J Cell Sci* 118, 5489-98.
- (19) Potente, M., Fisslthaler, B., Busse, R., and Fleming, I. (2003) 11,12-Epoxyeicosatrienoic acid-induced inhibition of FOXO factors promotes endothelial proliferation by down-regulating p27Kip1. *J Biol Chem* 278, 29619-25.
- (20) Sun, J., Sui, X., Bradbury, J. A., Zeldin, D. C., Conte, M. S., and Liao, J. K. (2002) Inhibition of vascular smooth muscle cell migration by cytochrome p450 epoxygenase-derived eicosanoids. *Circ Res* 90, 1020-7.
- (21) Imig, J. D. (2005) Epoxide hydrolase and epoxygenase metabolites as therapeutic targets for renal diseases. *Am J Physiol Renal Physiol* 289, F496-503.
- (22) Liu, Y., Zhang, Y., Schmelzer, K., Lee, T. S., Fang, X., Zhu, Y., Spector, A. A., Gill, S., Morisseau, C., Hammock, B. D., and Shyy, J. Y. (2005) The antiinflammatory effect of laminar flow: the role of PPARgamma, epoxyeicosatrienoic acids, and soluble epoxide hydrolase. *Proc Natl Acad Sci U S A* 102, 16747-52.
- (23) Schmelzer, K. R., Kubala, L., Newman, J. W., Kim, I. H., Eiserich, J. P., and Hammock, B. D. (2005) Soluble epoxide hydrolase is a therapeutic target for acute inflammation. *Proc Natl Acad Sci U S A* 102, 9772-7.
- (24) Ohtoshi, K., Kaneto, H., Node, K., Nakamura, Y., Shiraiwa, T., Matsuhisa, M., and Yamasaki, Y. (2005) Association of soluble epoxide hydrolase gene polymorphism with insulin resistance in type 2 diabetic patients. *Biochem Biophys Res Commun* 331, 347-50.

- (25) Zhang, W., Koerner, I. P., Noppens, R., Grafe, M., Tsai, H. J., Morisseau, C., Luria, A., Hammock, B. D., Falck, J. R., and Alkayed, N. J. (2007) Soluble epoxide hydrolase: a novel therapeutic target in stroke. *J Cereb Blood Flow Metab.*
- (26) Morisseau, C., Newman, J. W., Tsai, H. J., Baecker, P. A., and Hammock, B. D. (2006) Peptidyl-urea based inhibitors of soluble epoxide hydrolases. *Bioorg Med Chem Lett* 16, 5439-44.
- (27) Morisseau, C., Goodrow, M. H., Newman, J. W., Wheelock, C. E., Dowdy, D. L., and Hammock, B. D. (2002) Structural refinement of inhibitors of urea-based soluble epoxide hydrolases. *Biochem Pharmacol* 63, 1599-608.
- (28) Morisseau, C., and Hammock, B. D. (2005) Epoxide hydrolases: mechanisms, inhibitor designs, and biological roles. *Annu Rev Pharmacol Toxicol* 45, 311-33.
- (29) Arand, M., Cronin, A., Oesch, F., Mowbray, S. L., and Jones, T. A. (2003) The telltale structures of epoxide hydrolases. *Drug Metab Rev* 35, 365-83.
- (30) Pace-Asciak, C. R., and Lee, W. S. (1989) Purification of hepoxilin epoxide hydrolase from rat liver. *J Biol Chem* 264, 9310-3.
- (31) Nigam, S., Zafiriou, M. P., Deva, R., Ciccoli, R., and Roux-Van der Merwe, R. (2007) Structure, biochemistry and biology of hepoxilins: an update. *Febs J* 274, 3503-12.
- (32) Laneuville, O., Corey, E. J., Couture, R., and Pace-Asciak, C. R. (1991) Hepoxilin A3 (HxA3) is formed by the rat aorta and is metabolized into HxA3-C, a glutathione conjugate. *Biochim Biophys Acta* 1084, 60-8.
- (33) Pace-Asciak, C. R., and Martin, J. M. (1984) Hepoxilin, a new family of insulin secretagogues formed by intact rat pancreatic islets. *Prostaglandins Leukot Med* 16, 173-80.
- (34) Reynaud, D., Demin, P. M., Sutherland, M., Nigam, S., and Pace-Asciak, C. R. (1999) Hepoxilin signaling in intact human neutrophils: biphasic elevation of intracellular calcium by unesterified hepoxilin A3. *FEBS Lett* 446, 236-8.

- (35) Derewlany, L. O., Pace-Asciak, C. R., and Radde, I. C. (1984) Hepoxilin A, hydroxyepoxide metabolite of arachidonic acid, stimulates transport of ^{45}Ca across the guinea pig visceral yolk sac. *Can J Physiol Pharmacol* 62, 1466-9.
- (36) Carlen, P. L., Gurevich, N., Zhang, L., Wu, P. H., Reynaud, D., and Pace-Asciak, C. R. (1994) Formation and electrophysiological actions of the arachidonic acid metabolites, hepoxilins, at nanomolar concentrations in rat hippocampal slices. *Neuroscience* 58, 493-502.
- (37) Pace-Asciak, C. R., Laneuville, O., Su, W. G., Corey, E. J., Gurevich, N., Wu, P., and Carlen, P. L. (1990) A glutathione conjugate of hepoxilin A3: formation and action in the rat central nervous system. *Proc Natl Acad Sci U S A* 87, 3037-41.
- (38) Anton, R., Puig, L., Esgleyes, T., de Moragas, J. M., and Vila, L. (1998) Occurrence of hepoxilins and trioxilins in psoriatic lesions. *J Invest Dermatol* 110, 303-10.
- (39) Mrsny, R. J., Gewirtz, A. T., Siccardi, D., Savidge, T., Hurley, B. P., Madara, J. L., and McCormick, B. A. (2004) Identification of hepoxilin A3 in inflammatory events: a required role in neutrophil migration across intestinal epithelia. *Proc Natl Acad Sci U S A* 101, 7421-6.
- (40) McCormick, B. A. (2007) Bacterial-induced hepoxilin A3 secretion as a pro-inflammatory mediator. *Febs J* 274, 3513-8.
- (41) Brash, A. R., Yu, Z., Boeglin, W. E., and Schneider, C. (2007) The hepoxilin connection in the epidermis. *Febs J* 274, 3494-502.
- (42) Laneuville, O., Corey, E. J., Couture, R., and Pace-Asciak, C. R. (1991) Hepoxilin A3 increases vascular permeability in the rat skin. *Eicosanoids* 4, 95-7.
- (43) Epp, N., Furstenberger, G., Muller, K., de Juanes, S., Leitges, M., Hausser, I., Thieme, F., Liebisch, G., Schmitz, G., and Krieg, P. (2007) 12R-lipoxygenase deficiency disrupts epidermal barrier function. *J Cell Biol* 177, 173-82.

- (44) Yu, Z., Schneider, C., Boeglin, W. E., and Brash, A. R. (2007) Epidermal lipoxygenase products of the hepoxilin pathway selectively activate the nuclear receptor PPARalpha. *Lipids* 42, 491-7.
- (45) Furstenberger, G., Epp, N., Eckl, K. M., Hennies, H. C., Jorgensen, C., Hallenborg, P., Kristiansen, K., and Krieg, P. (2007) Role of epidermis-type lipoxygenases for skin barrier function and adipocyte differentiation. *Prostaglandins Other Lipid Mediat* 82, 128-34.
- (46) Yu, Z., Schneider, C., Boeglin, W. E., and Brash, A. R. (2005) Mutations associated with a congenital form of ichthyosis (NCIE) inactivate the epidermal lipoxygenases 12R-LOX and eLOX3. *Biochim Biophys Acta* 1686 3, 238-47.
- (47) Sutherland, M., Schewe, T., and Nigam, S. (2000) Biological actions of the free acid of hepoxilin A3 on human neutrophils. *Biochem Pharmacol* 59, 435-40.
- (48) Reynaud, D., Demin, P., and Pace-Asciak, C. R. (1996) Hepoxilin A3-specific binding in human neutrophils. *Biochem J* 313 (Pt 2), 537-41.
- (49) Nigam, S., Nodes, S., Cichon, G., Corey, E. J., and Pace-Asciak, C. R. (1990) Receptor-mediated action of hepoxilin A3 releases diacylglycerol and arachidonic acid from human neutrophils. *Biochem Biophys Res Commun* 171, 944-8.
- (50) Marowsky, A., Burgener, J., Falck, J. R., Fritschy, J. M., and Arand, M. (2009) Distribution of soluble and microsomal epoxide hydrolase in the mouse brain and its contribution to cerebral epoxyeicosatrienoic acid metabolism. *Neuroscience* 163, 646-61.
- (51) Sinal, C. J., Miyata, M., Tohkin, M., Nagata, K., Bend, J. R., and Gonzalez, F. J. (2000) Targeted disruption of soluble epoxide hydrolase reveals a role in blood pressure regulation. *J Biol Chem* 275, 40504-10.

- (52) Hwang, S. H., Tsai, H. J., Liu, J. Y., Morisseau, C., and Hammock, B. D. (2007) Orally bioavailable potent soluble epoxide hydrolase inhibitors. *J Med Chem* 50, 3825-40.
- (53) Schladt, L., Hartmann, R., Worner, W., Thomas, H., and Oesch, F. (1988) Purification and characterization of rat-liver cytosolic epoxide hydrolase. *Eur J Biochem* 176, 31-7.
- (54) Arand, M., Knehr, M., Thomas, H., Zeller, H. D., and Oesch, F. (1991) An impaired peroxisomal targeting sequence leading to an unusual bicompartmental distribution of cytosolic epoxide hydrolase. *FEBS Lett* 294, 19-22.
- (55) Mullen, R. T., Trelease, R. N., Duerk, H., Arand, M., Hammock, B. D., Oesch, F., and Grant, D. F. (1999) Differential subcellular localization of endogenous and transfected soluble epoxide hydrolase in mammalian cells: evidence for isozyme variants. *FEBS Lett* 445, 301-5.

Tables and Figures

Figure 1: Biosynthesis and metabolism of hepoxilins. Hepoxilins are synthesised from arachidonic acid by the action of 12S-lipoxygenase (12S-LOX) and epidermis-type lipoxygenase 3 (eLOX-3), leading to the regioisomers hepoxilin A₃ and B₃. The hepoxilins are turned over by sEH to the corresponding trihydroxy metabolites TrxA₃ and B₃. (Note that in the skin a specific 12R-LOX generates hepoxilins with R-configuration. This pathway plays a role in epidermal differentiation and skin barrier function.)

Figure 2: Kinetic analysis of hepoxilin turnover by sEH. Human and rat sEH were cloned, recombinantly expressed in *E.coli* and purified as described above. Purified enzymes were incubated with various concentrations of substrate and samples were analysed by LC-MS/MS. Substrate turnover was determined using internal HxA₃ and HxB₃ standards and the quantification function of the Analyst software 4.2.1. Kinetic constants were calculated by simulation of the Michaelis Menten kinetic as described in the experimental section.

Figure 3: Gel Permeation Chromatographie. 5 mg mouse liver cytosol was separated on a SE-1000 gel permeation column (Amersham biosciences) in phosphate buffered saline, pH 7.4. Each elution fraction was assayed for the metabolism of HxA₃, 14,15-EET and 5,6-EET (600 nM) as described in the experimental section. Each fraction was further analysed for the presence of sEH protein by western blot (lower panel).

Figure 4: Inhibition of sEH. Rat and human sEH were incubated with 3 μ M HxA₃ and HxB₃ in the presence of sEH selective inhibitors (2 μ M ACU, 2 μ M AUDA) and samples were analysed by LC-MS/MS as described in the experimental section. Bars represent the amount of hepoxilin formed by sEH in the presence of inhibitors compared to the control without

inhibitor. The inserted representations show the structures of the sEH inhibitors ACU (1-Adamantyl-3-cyclohexylurea) and AUDA (12-(3-adamantan-1-yl-ureido)-dodecanoic acid).

Figure 5: Inhibition of hepoxilin metabolism. Protein extracts from liver (cytosolic and microsomal preparations) of WT mice were incubated with 3 μM HxA₃ and HxB₃ in the presence of inhibitors (2 μM ACU, AUDA, 2 mM valpromide), and samples were analysed by LC-MS/MS. The representations show the fraction (%) of substrate turnover compared to the cytosolic preparation of WT animals which is adjusted to 100% turnover. Error bars indicate the standard deviation. Unpaired, one-sided Student's *t*-tests were performed on each set of inhibited versus non inhibited samples. Two stars indicate a significant statistical difference with a p-value < 0.01.

Figure 6: Hepoxilin metabolism by sEH in WT and sEH^{-/-} mice. Protein extracts (50 μg) from liver (cytosolic and microsomal preparations) of sEH^{-/-} and WT mice were incubated with 3 μM HxA₃ and HxB₃, and samples were analysed by LC-MS/MS. The representations show the fraction (%) of substrate turnover compared to the cytosolic preparation of WT animals which is adjusted to 100% turnover. Error bars indicate the standard deviation. Unpaired, one-sided Student's *t*-tests were performed on each set of samples from WT versus KO animals. Two stars indicate a significant statistical difference with a p-value < 0.01.

Figure 7: Lipid extracts. **a)** Levels of hepoxilins and trioxilins in liver extracts of WT and sEH^{-/-} mice. Liver samples of sEH WT and sEH^{-/-} animals were homogenized, adjusted to a final concentration of 20% ethanol and lipids were isolated by solid phase extraction. **b)** Levels of hepoxilins and trioxilins in liver extracts of WT and sEH^{-/-} mice upon stimulation with exogenous arachidonic acid. Liver samples of sEH WT and sEH^{-/-} animals were homogenized and treated with 30 μM arachidonic acid for 30 min. Samples were adjusted to a

final concentration of 20% ethanol and lipids were isolated by solid phase extraction. Samples were analysed for hepoxilin metabolism by LC-MS/MS. The values are presented in pmol lipid per g tissue. Error bars indicate the standard deviation. Unpaired, one-sided Student's *t*-tests were performed on each set of samples from WT versus KO animals. Two stars indicate a significant statistical difference with a p-value < 0.01.

Table 1. Summary of kinetic parameters for hepoxilin turnover by sEH.

sEH substrate	<i>V</i>_{max} <i>nmol/mg/min</i>	<i>K</i>_m <i>μM</i>	<i>k</i>_{cat} <i>s⁻¹</i>	<i>k</i>_{cat}/<i>K</i>_m <i>M⁻¹s⁻¹</i>
rsEH HxA ₃	1739 ± 539	4.6 ± 2.3	1.88 ± 0.58	4.5 x 10 ⁵ ± 1.6x10 ⁵
rsEH HxB ₃	550 ± 261	14.7 ± 5.3	0.60 ± 0.28	5.1 x 10 ⁴ ± 1.4 x 10 ⁴
hsEH HxA ₃	385 ± 95	7.3 ± 3.3	0.42 ± 0.10	5.8 x 10 ⁴ ± 9.5 x 10 ³
hsEH HxB ₃	95 ± 43	10.8 ± 3.4	0.10 ± 0.05	1.2 x 10 ⁴ ± 8.4 x 10 ³

Kinetic constants were calculated by simulation of the Michaelis Menten kinetic as described in the experimental section. Variations were calculated from 4-5 independent experiments.

Figure 1

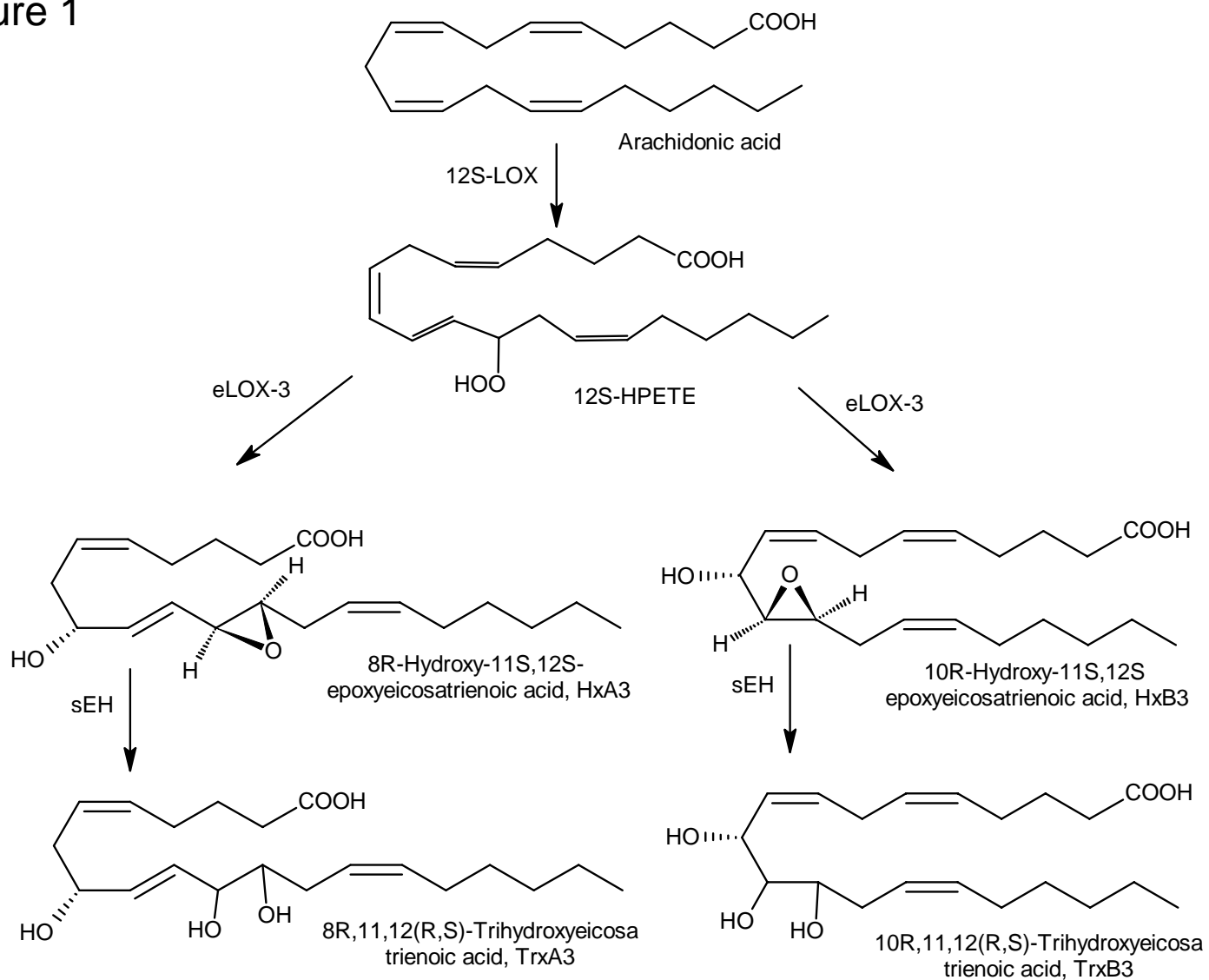


Figure 2

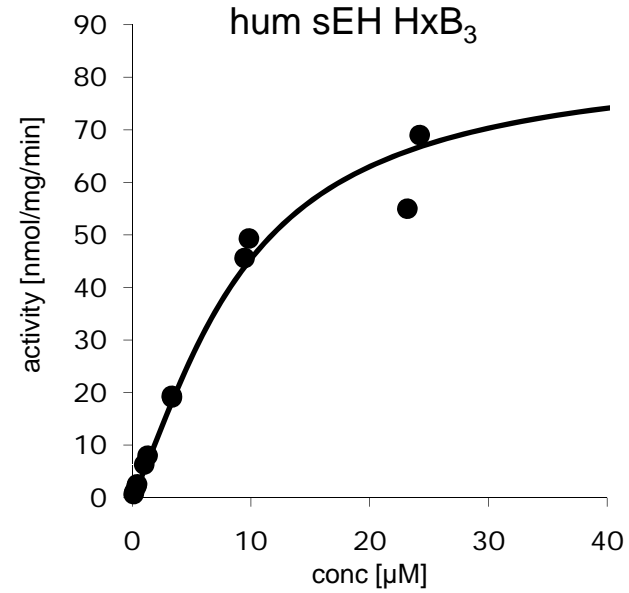
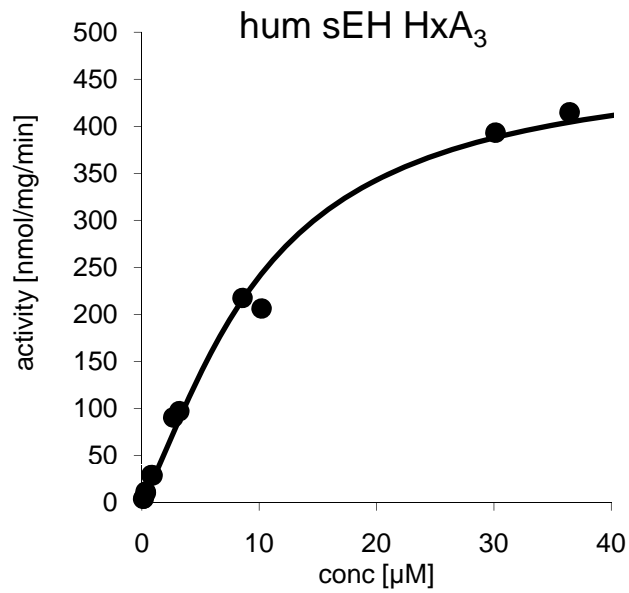
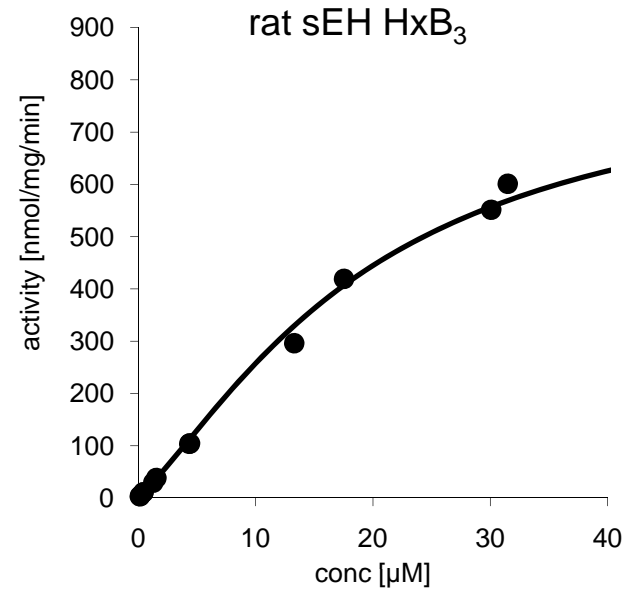
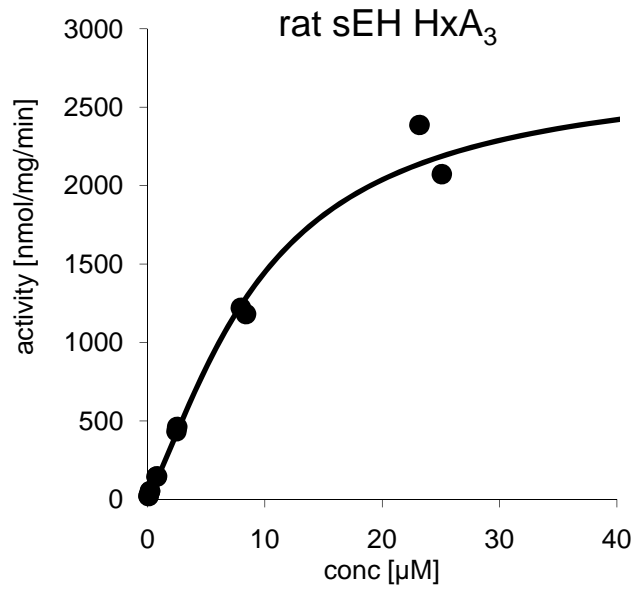


Figure 3

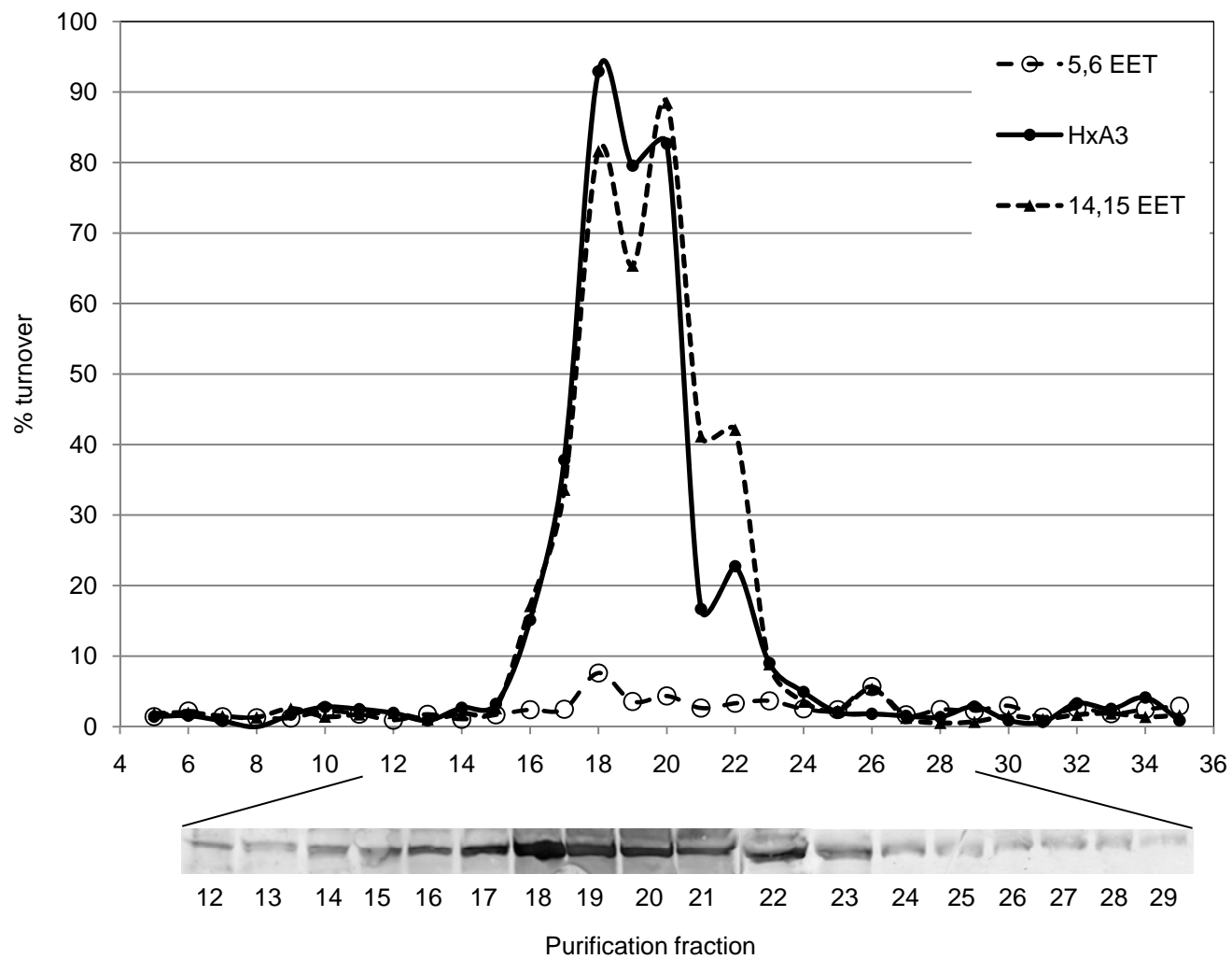


Figure 4

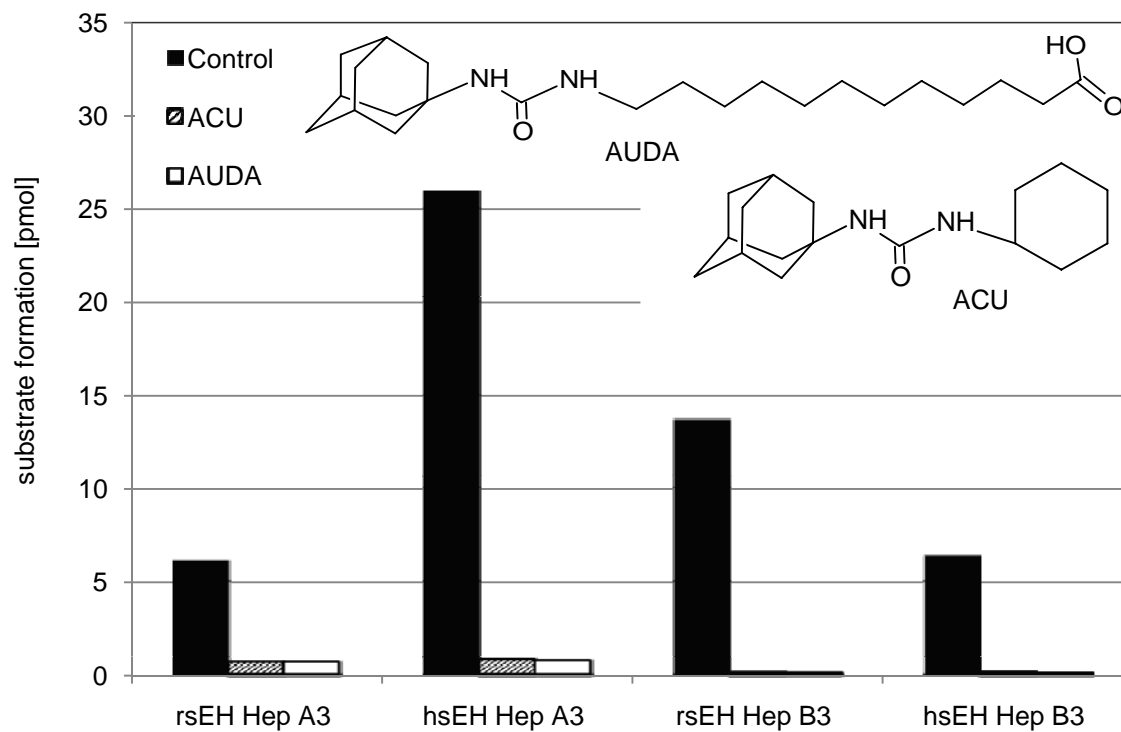


Figure 5

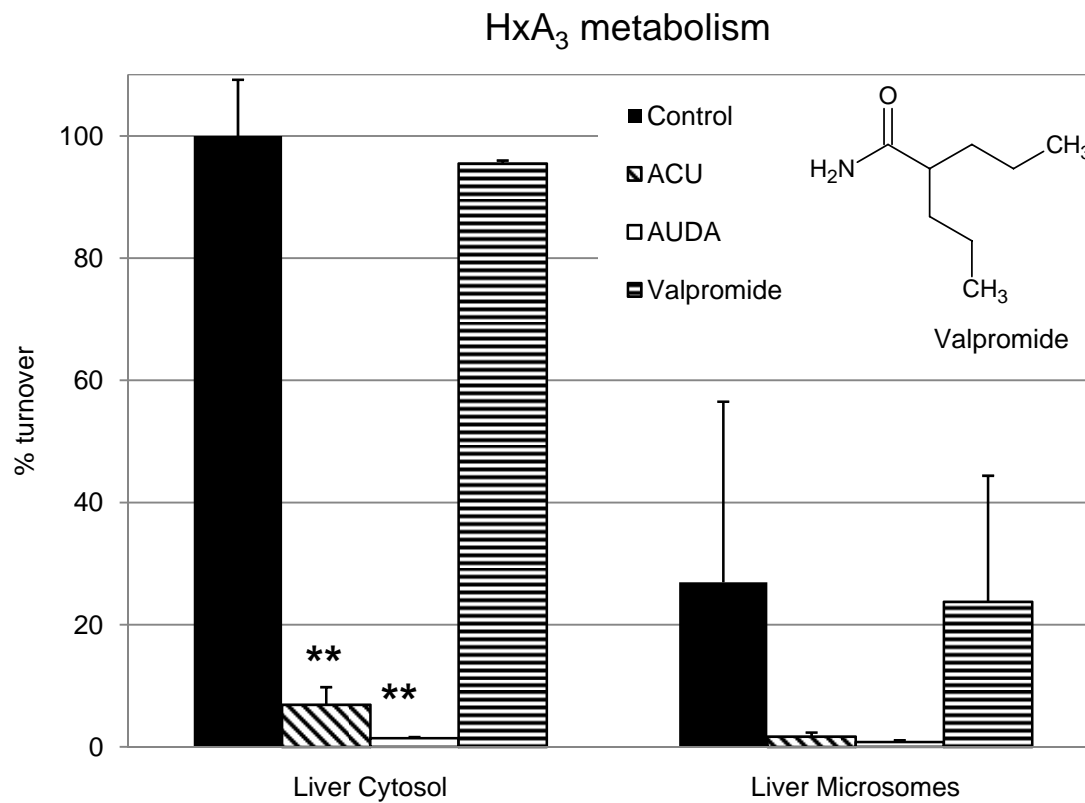


Figure 6

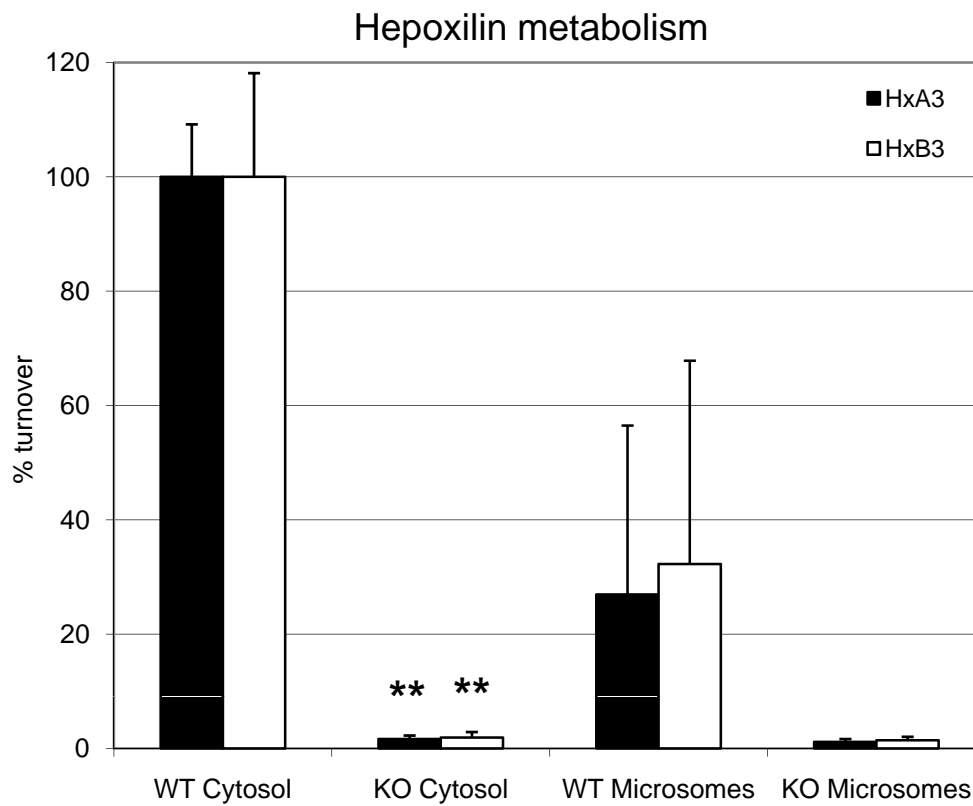


Figure 7

